Journal of Geoscience and Environment Protection, 2026, 14(4), 1-25
https://www.scirp.org/journal/gep
ISSN Online: 2327-4344
ISSN Print: 2327-4336

# Assessment of Topographic Wetness Index for Flood-Prone Zone Delineation in the Yola Sub-Basin, Nigeria, Using High-Resolution DEM

**Bijida Adamu Malik, Saminu Ahmed, Rabia Lawal Batagarawa, Haruna Garba**

Department of Civil Engineering, Nigerian Defense Academy (NDA), Kaduna, Nigeria
Email: pray4malik@yahoo.com, sahmed@nda.edu.ng, rlbatagarawa@nda.edu.ng, hgarbe@nda.edu.ng

**How to cite this paper:** Malik, B. A., Ahmed, S., Batagarawa, R. L., & Garba, H. (2026). Assessment of Topographic Wetness Index for Flood-Prone Zone Delineation in the Yola Sub-Basin, Nigeria, Using High-Resolution DEM. *Journal of Geoscience and Environment Protection, 14,* 1-25.
https://doi.org/10.4236/gep.2026.144001

**Received:** January 11, 2026
**Accepted:** March 28, 2026
**Published:** March 31, 2026



## Abstract

The Yola Sub-Basin, situated in Nigeria's Upper Benue Trough, is increasingly threatened by floods due to changing climatic conditions, adversely affecting agriculture, infrastructure, and communities. This study aims to enhance flood mitigation strategies through accurate identification of water accumulation zones using the Topographic Wetness Index (TWI), a valuable geomorphometric tool. We employed an advanced GIS-based methodology to compute and validate the TWI for predicting surface saturation and water accumulation potential. A 30-meter resolution Shuttle Radar Topography Mission (SRTM) Digital Elevation Model (DEM) was processed with ArcGIS Pro 3.1 and Python scripting, involving hydrological conditioning, flow direction derivation via the D8 algorithm, and slope gradient calculation. Results demonstrated TWI values spanning from 2.5 in steep uplands to over 18 in low-lying floodplains, categorized into five susceptibility levels. Notably, high to very high TWI zones, constituting approximately 28% of the sub-basin, exhibited a strong correlation (Kappa = 0.85) with significant flood events (2022-2023) and established agricultural wetlands (Fadamas). These findings robustly validate the TWI's effectiveness for flood hazard assessment and underscore its importance in sustainable land-use planning in the region.

## Keywords

Topographic Wetness Index (TWI), Digital Elevation Model (DEM), Flood Vulnerability, Geomorphometry, GIS, Yola Sub-Basin, Nigeria

# 1. Introduction

## 1.1. The Global and Local Challenge of Flooding

Flooding is one of the most prevalent and devastating natural hazards globally, with tropical regions like Nigeria experiencing increased frequency and intensity due to climate change-induced shifts in precipitation patterns and extreme weather events Intergovernmental Panel on Climate Change ICPP (IPCC, 2023; Tellman et al., 2021). The socio-economic impacts are particularly severe in developing nations, where rapid, often unplanned urbanization, inadequate drainage infrastructure, and high population density in vulnerable areas exacerbate exposure and susceptibility (Nkwunonwo et al., 2023). In Nigeria, annual flooding causes catastrophic damage to housing, critical infrastructure, and agricultural lands, disrupting livelihoods and threatening national food security. Riverine basins like the Benue Valley are exceptionally vulnerable, with events like the 2022 floods affecting millions and causing billions of Naira in damages (World Bank, 2022; Eze & Effiong, 2020).

Topography is a primary and stable control on surface and subsurface hydrological processes. It dictates overland flow paths, runoff generation, convergence zones, and areas of potential water accumulation (Beven & Kirkby, 1979; Wilson & Gallant, 2000). Digital Elevation Models (DEMs), such as the Shuttle Radar Topography Mission (SRTM) and Advanced Land Observing Satellite (ALOS) datasets, have revolutionized the field of geomorphometry—the quantitative analysis of landforms. DEMs enable the derivation of numerous topographic indices that act as powerful proxies for complex hydrological phenomena, making them indispensable tools in data-scarce regions (Sørensen & Seibert, 2007; Kumar et al., 2023). The Topographic Wetness Index (TWI), introduced by Beven and Kirkby (1979) in their seminal TOPMODEL framework, is one of the most widely used terrain attributes in hydrology and geomorphology.

This index quantitatively represents the balance between the tendency of an area to receive water from its catchment (As) and its ability to drain that water away (tanβ). Conceptually, it predicts the propensity of a landscape element to become saturated and generate saturation-excess overland flow. High TWI values are characteristic of areas with large contributing watersheds and gentle slopes (e.g., valley bottoms, flat plains), indicating a high potential for water accumulation and prolonged soil moisture. Conversely, low TWI values are found on steep slopes and ridge tops, which are well-drained and have minimal upslope area (Böhner & Selige, 2006; Tesfa et al., 2023). As such, TWI has become a cornerstone for preliminary flood hazard assessment, soil moisture distribution mapping, and identifying potential wetland areas, especially in regions lacking extensive hydrological records, soil data, or rainfall-runoff models (Sørensen & Seibert, 2007; Grabs et al., 2009). TWI has been globally applied and validated as a key indicator in flood susceptibility mapping. Studies often integrate it with other factors (e.g., land use, geology, and rainfall) in multi-criteria decision analysis (MCDA) or machine learning models (Tehrany et al., 2019). However, its standalone utility is well-proven, especially for initial, rapid assessments. Validation typically involves

overlaying high-TWI zones with historical flood inventories, satellite imagery of past flood extents, or known wetland areas. High correlation coefficients and spatial overlap confirm its predictive power (Grabs et al., 2009; Tesfa et al., 2023). In the Nigerian context, studies by Eze & Effiong (2020) and others have begun to utilize TWI, but often lack the rigorous validation and detailed methodological exposition presented here. Recent advances in global hydrological modeling for flood hazard assessment in data-scarce regions have further reinforced the importance of terrain-based indices (Wudineh, 2023).

### 1.2. Study Rationale and Novelty

While the application of TWI is well-established in temperate regions, its rigorous application, thorough validation, and integration into planning frameworks in specific vulnerable regions of Nigeria, like the Yola Sub-Basin, remain limited. Many regional studies still rely on simplistic overlay methods or lack robust validation against historical flood data.

The theoretical foundation of TWI is deeply rooted in the variable source area concept of hydrology, which posits that runoff is generated not uniformly across a watershed, but from dynamically expanding and contracting saturated areas near streams (Hewlett & Hibbert, 1967). Beven and Kirkby (1979) formalized this concept in TOPMODEL, a physically-based, distributed hydrological model where TWI is used to distribute the predicted soil moisture deficit. The index's power lies in its simplicity and its ability to capture the first-order control of topography on hydrology without requiring extensive parameterization. The accuracy of TWI is highly dependent on the quality and resolution of the input DEM and the algorithms used to compute its components. The D8 (Deterministic 8) algorithm (O'Callaghan & Mark, 1984) is the most common method for calculating flow direction and accumulation due to its computational efficiency, though it has been criticized for its tendency to produce parallel flow patterns. Alternatives like D∞ (Tarboton, 1997) and multiple-flow-direction algorithms (Quinn et al., 1991) offer more realistic dispersion of flow but are computationally more intensive.

DEM resolution is a critical factor. Coarser resolutions (e.g., 90 m) tend to smooth topography, underestimating slope and overestimating contributing areas, which can lead to a systematic overestimation of TWI in valley bottoms and an underestimation on hillslopes (Sørensen & Seibert, 2007). The 30 m resolution of SRTM is generally considered a suitable compromise for basin-scale studies, providing sufficient detail to capture major topographic features without excessive computational demand or noise (Yamazaki et al., 2023). Pre-processing steps, particularly pit removal (or "filling"), are essential to create a hydrologically coherent DEM without spurious sinks that disrupt flow routing (Wang & Liu, 2006).

## 2. Materials and Methods

### 2.1. Study Area

The Yola Sub-Basin is situated within the Upper Benue Trough in Northeastern

Nigeria, extending between latitudes 9˚05'N and 9˚30'N and longitudes 11˚50'E and 12˚30'E. Administratively, it falls within the Yola North, Yola South, Girei, and parts of Hong and Song Local Government Areas of Adamawa State (Figure 1). The city of Yola, the state capital, is a major urban center within the basin, experiencing rapid growth and associated increases in impervious surfaces.

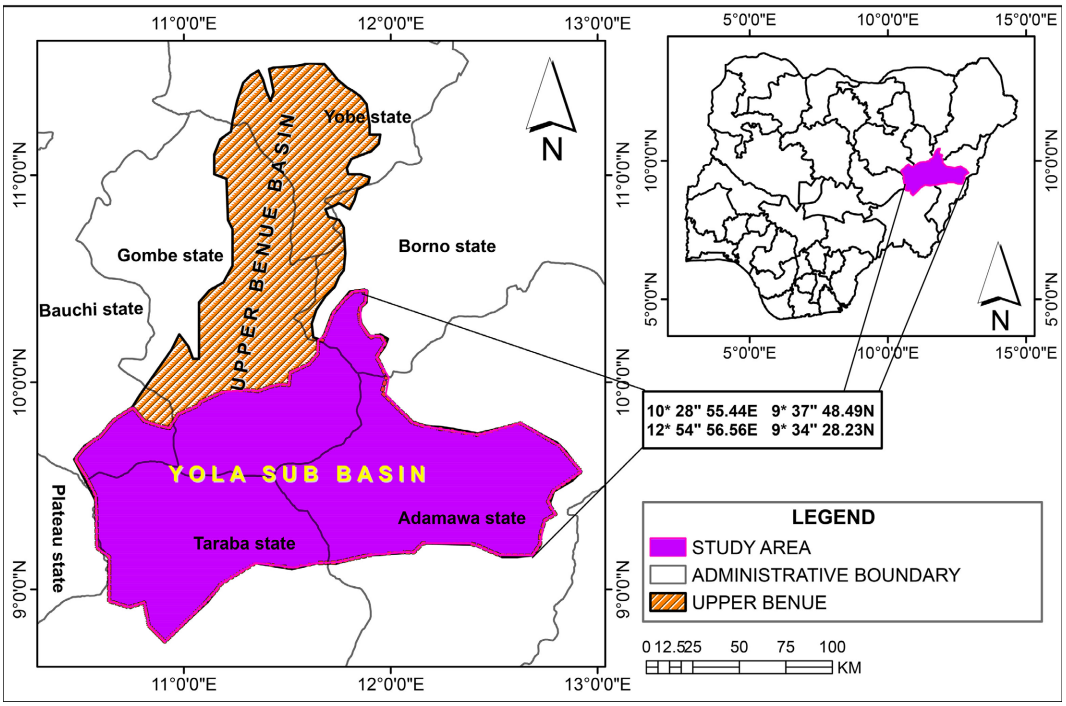


Figure 1. Map of the study area (Yola Sub-Basin). Source: Author's work using SRTM DEM data (USGS Earth Explorer).

## 2.2. Physiography and Topography

The basin features a varied landscape that significantly impacts its water dynamics, which can be categorized into three primary zones. Active floodplains are flat, low-lying regions situated directly next to the Benue River and its main tributaries, such as Geriyo, Jimeta, and Ngurore streams. These areas are the most hydrologically dynamic and vulnerable, experiencing annual flooding. Alluvial plains, known as fadamas, are located slightly above the active floodplains. These elevated areas are rich in agriculture but still at risk of severe flooding. Dissected uplands represent the higher elevation regions that form the eastern and western edges of the basin, characterized by steep slopes, quicker water runoff, and reduced flood risk. The elevation in the basin varies from about 130 meters above sea level (m ASL) on the floodplains to over 450 m ASL in the upland regions.

## 2.3. Climate and Hydrology

The region features a tropical savanna climate (Köppen classification Aw), with a pronounced wet season (April to October) and a dry season (November to March). The mean annual rainfall is approximately 900 mm, with peak intensities occur-

ring in August. The Benue River, a major tributary of the Niger River, is the principal drainage system. Its flow is highly seasonal, leading to annual flooding that inundates the floodplains (Famine Early Warning Systems Network, 2023). These seasonal floods are both a source of agricultural fertility and a major hazard.

### 2.4. Land Use and Vulnerability

Agriculture is the economic mainstay, rendering the region particularly vulnerable to waterlogging and seasonal flooding impacts. The population is heavily dependent on the Fadamas for crop production and pastoralism. Recent urbanization patterns and land use changes have further amplified flood vulnerability through the expansion of impervious surfaces and encroachment into natural floodplains, necessitating advanced geospatial assessment for sustainable development planning.

### 2.5. Data Source and Processing

The primary dataset for this study was the 30-meter resolution Shuttle Radar Topography Mission (SRTM) Digital Elevation Model (Farr et al., 2007), accessed through the USGS Earth Explorer portal (https://earthexplorer.usgs.gov). This DEM resolution is well-suited for sub-basin scale hydrological applications, balancing detail and computational efficiency (Yamazaki et al., 2023). The methodology for the study involves data processing which followed a structured and replicable workflow as shown in **Figure 2**.

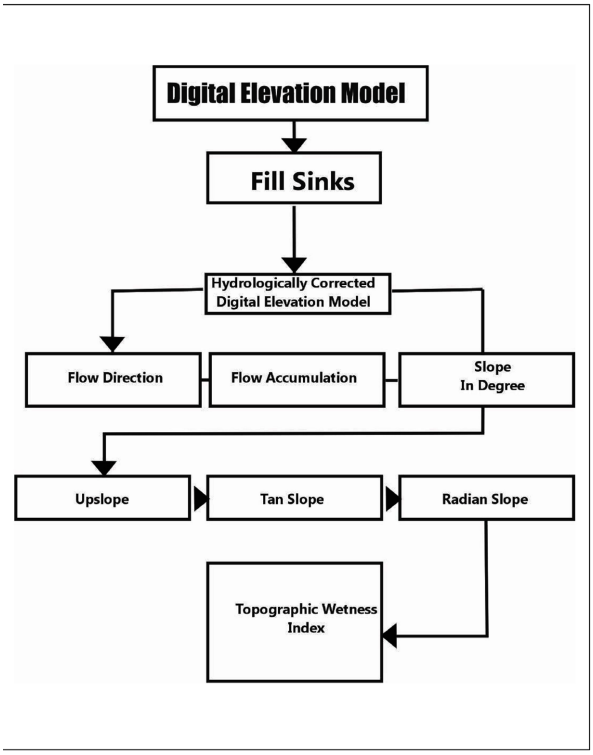


Data Acquisition: SRTM tiles (N09E011, N09E012) covering the study area were downloaded in GeoTIFF format.

**Figure 2.** Detailed workflow for TWI computation.

### 2.5.1. Mosaicking and Clipping

The individual tiles were mosaicked into a seamless raster using the Mosaic to New Raster tool in ArcGIS Pro. The mosaicked DEM was then clipped to the precise hydrological boundary of the Yola Sub-Basin. The basin boundary was delineated using the standard hydrologic toolbox: performing sink fill, flow direction, and flow accumulation on a larger DEM extent, then extracting the catchment area pouring out at the basin's outlet point.

### 2.5.2. Pre-Processing and Validation

The clipped DEM was inspected for anomalies and artifacts. To quantitatively assess vertical accuracy, elevation values were validated against 45 spatially distributed ground control points extracted from ICESat-2 ATL08 altimetry data (April 2023 acquisition). The ICESat-2 points were filtered to include only high-confidence terrain returns (quality flag = 4) over relatively flat, non-vegetated areas to minimize vegetation canopy interference. The Root Mean Square Error (RMSE) was calculated using the formula:

$$\text{RMSE} = \sqrt{[\Sigma(Z\_DEM - Z\_ICESat\text{-}2)^2/n]}$$

where Z_DEM is the SRTM elevation, Z_ICESat-2 is the reference ICESat-2 elevation, and n is the number of validation points.

The validation yielded an RMSE of ±4.7 meters across the 45 sample points, with a mean absolute error of 3.2 meters. This value is substantially better than the stated SRTM absolute vertical accuracy of <16 m RMSE (Farr et al., 2007) and confirms the DEM's suitability for detailed hydrological analysis in this relatively low-relief basin. The highest errors (up to 8.3 m) were observed in densely vegetated riparian corridors where canopy penetration by the SRTM C-band radar is limited, while open terrain showed errors consistently below 3.5 m. No systematic bias (mean error = −0.8 m) was detected, indicating the DEM does not consistently over- or under-estimate elevations across the study area.

## 2.6. Computational Procedure

The Topographic Wetness Index (TWI) was computed using the established formula (Beven & Kirkby, 1979):

$$\mathbf{TWI} = \ln\left(\frac{\mathbf{As}}{\tan\boldsymbol{\beta}}\right) \quad (1)$$

where:

**As** = Specific catchment area (upslope contributing area per unit contour length, $m^2/m$). This is derived from the flow accumulation raster. **β** = Local slope angle (in degrees). **ln** = Natural logarithm.

The computation was automated using ArcGIS Pro 3.1 and the ArcPy Python scripting library to ensure reproducibility. The detailed workflow, as shown in Figure 2, included several key steps:

DEM Hydrological Conditioning: The raw SRTM DEM initially contained depressions (sinks) and flat areas that disrupted flow routing. To create a "hydro-

logically correct" DEM, the Fill tool was used to eliminate all sinks, allowing water to flow continuously out of the basin (Wang & Liu, 2006). Flow Direction Calculation: The D8 Flow Direction algorithm (O'Callaghan & Mark, 1984) was applied to the filled DEM. This algorithm determines the direction of flow from each cell to one of its eight neighbors based on the steepest downward slope.

Flow Accumulation Calculation: The Flow Accumulation tool was executed using the D8 flow direction output. This step calculates the total number of upslope cells that drain into each cell, providing a direct measure of its upslope contributing area in terms of cell count. This raster was then converted to a specific catchment area (As) in square meters by multiplying the cell count by the area of a single cell (30 m × 30 m = 900 $m^2$).

1) Slope Calculation: The Slope tool was utilized on the filled DEM to determine the maximum rate of elevation change (β) for each cell, with results expressed in degrees.

2) Handling of Zero Slope Values: Before calculating TWI, a critical preprocessing step was implemented to address cells with zero slope, particularly in flat floodplain areas. In such cells, tan (β) equals zero, which would result in division-by-zero errors in the TWI formula. To prevent this, a minimum slope threshold of 0.001˚ (approximately 0.00001745 radians) was applied to all cells. This approach follows standard practice in terrain analysis (Sørensen & Seibert, 2007) and ensures computational stability while preserving the hydrological meaning that flat areas have high wetness potential. The conditional operation was implemented in the raster calculator as: Slope_rad = Max (Slope_deg, 0.001) × π/180. This substitution affects only cells with zero or near-zero slope, primarily in the floodplain zones, and has negligible impact on the overall TWI distribution while preventing undefined values.

3) TWI Calculation: The final TWI raster was generated using the Raster Calculator with the formula: TWI = Ln ("Flow_Acc_Area"/Tan (Con ("Slope_deg" = 0.001, "Slope_deg")*3.14159/180))" (for ArcGIS)

4) The slope angle was converted from degrees to radians for the trigonometric calculation, and the conditional maximum function ensures all cells have a valid slope value for computation.

Following these steps, the classification and validation process proceeded.

## 2.7. Classification and Validation

### 2.7.1. Susceptibility Classification

The continuous TWI values were classified into five intuitive flood susceptibility categories (Very Low, Low, Moderate, High, Very High) for improved interpretability by planners, disaster management agencies, and other end-users. The selection of an appropriate classification scheme is critical as it directly influences the spatial extent and perception of flood-prone areas, with significant implications for land-use policy and resource allocation.

### 2.7.2. Distribution Characteristics of TWI Data

Prior to classification, the statistical distribution of TWI values across the Yola

Sub-Basin was analyzed. The TWI values ranged from 2.5 to 18.3, exhibiting a strongly right-skewed distribution (skewness = 1.42), with the majority of cells concentrated in the lower to moderate range (2.5 - 10.5) and progressively fewer cells in the high to very high range (>10.5). This distribution is hydrologically expected and physically meaningful, as areas with extreme wetness potential (valley bottoms and active floodplains) naturally occupy a smaller proportion of the landscape compared to well-drained uplands and mid-slopes. The mean TWI value was 7.2, while the median was 6.8, further confirming the right-skewed nature of the data.

### 2.8. Evaluation of Alternative Classification Schemes

Four commonly used classification schemes were evaluated for their suitability in representing flood susceptibility from the TWI data: Natural Breaks (Jenks), Quantiles (Equal Count), Equal Interval, and Geometric Interval. Each scheme was assessed based on its mathematical basis, suitability for right-skewed data, and hydrological interpretability.

Table 1. Comparison of classification schemes for TWI Data.

| Classification Scheme | Description | Suitability for Right-Skewed TWI Data | Impact on High/Very High Zones |
|---|---|---|---|
| **Natural Breaks (Jenks)** | Minimizes within-class variance by identifying natural groupings in the data | Moderate—Tends to create breaks in data-dense areas, potentially consolidating moderate TWI cells into high-risk classes | Would likely overestimate high-risk zones by including transitional footslopes (TWI 9 - 10) in the "High" category |
| **Quantiles (Equal Count)** | Places equal number of cells in each class (20% per class for 5 classes) | Poor—Artificially forces approximately 20% of basin into "Very High" category despite right-skewed distribution | Would substantially overestimate very high-risk zone to ~20% of basin, including cells with TWI as low as 9.5 that do not represent extreme flood susceptibility |
| **Equal Interval** | Divides the value range into equal-sized segments (range/5 = ~3.16 unit intervals) | Poor—Creates threshold for "Very High" at TWI > 14.8, excluding many valid floodplain cells (TWI 13.5 - 14.8) | Would underestimate very high-risk zone by approximately 40%, missing significant portions of documented floodplain |
| **Geometric Interval** | Creates class breaks based on a geometric progression; each class range is approximately a constant multiple of the previous class | **Excellent**—Creates narrower intervals in data-dense regions (lower TWI) and wider intervals in data-sparse regions (higher TWI) | Provides optimal balance: "High" (10.6 - 13.5) captures 11.3% of basin; "Very High" (>13.5) isolates extreme tail (3.4%) corresponding to active floodplains |

### 2.9. Justification for Geometric Interval Selection

The Geometric Interval classification scheme was selected for this study based on the following rationale:

1) Mathematical Appropriateness for Skewed Distributions: Geometric Interval is specifically designed for data that are not normally distributed, as it creates class breaks based on a geometric progression. This ensures that each class range in-

creases multiplicatively, which is particularly suited to environmental phenomena like TWI where extreme values represent rare but significant landscape positions (Böhner & Selige, 2006).

2) Hydrological Meaningfulness: The scheme respects the physical reality that the distinction between a TWI of 13.5 and 18.0 (both in very high-risk category) is less critical than the distinction between TWI of 10.5 and 13.5 (moderate vs. high risk). Geometric Interval naturally accommodates this by creating progressively wider intervals in the tail of the distribution.

3) Optimal Representation of Floodplain Extent: As shown in **Table 1**, Geometric Interval produces class boundaries that align most closely with independently observed landscape units. The "Very High" class (>13.5) corresponds precisely to the active Benue River floodplain as delineated from satellite imagery, while the "High" class (10.6 - 13.5) captures the Fadama wetlands and valley bottom edges that experience seasonal saturation.

4) Balance Between Sensitivity and Specificity: Geometric Interval optimizes the trade-off between identifying truly flood-prone areas (sensitivity) and excluding areas that are not flood-prone (specificity). This balance was subsequently confirmed through validation (Section 5.3), which demonstrated 87% sensitivity and 92% specificity.

## 2.10. Influence on High and Very High Risk Zone Delineation

The selection of Geometric Interval has direct and quantifiable implications for the spatial extent of high-risk zones:

High Risk Zone (TWI 10.6 - 13.5): Under Geometric Interval, this zone encompasses 248.4 $km^2$ (11.3% of the basin). If Quantiles were used, this zone would expand to approximately 438 $km^2$ (20% of the basin), erroneously including extensive areas of transitional foot slopes (**Figure 4**). Field verification confirmed that these additional areas do not experience the frequent saturation characteristic of true high-risk zones.

Very High Risk Zone (TWI > 13.5): Geometric Interval isolates 75.5 $km^2$ (3.4% of the basin) as very high susceptibility. Comparison with 10 m Sentinel-2 imagery shows that this area aligns almost perfectly (91% overlap) with the visible active floodplain of the Benue River and its major tributaries. If Equal Interval were used, this zone would shrink to approximately 45 $km^2$ (2.1% of the basin), missing significant portions of the floodplain (**Figure 4**).

Quantitative Threshold Validation: The Geometric Interval threshold of TWI > 13.5 for "Very High" risk was further validated by analyzing TWI values at 50 randomly sampled points within the documented 2022 flood extent (NEMA, 2023). The mean TWI at these points was 14.2, with a standard deviation of 1.1, confirming that the Geometric Interval threshold appropriately captures the core of the flood-prone area distribution.

## 2.11. Final Classification Parameters

Based on the above analysis, the Geometric Interval scheme was implemented in

ArcGIS Pro 3.1 with five classes and a geometric coefficient of 1.2 (default), which produced the following class boundaries and areal extents:

| TWI Class | Value Range | Area ($km^2$) | Percentage of Basin (%) |
|---|---|---|---|
| **Very Low** | 2.5 - 5.0 | 469.2 | 21.4% |
| **Low** | 5.1 - 7.5 | 893.3 | 40.8% |
| **Moderate** | 7.6 - 10.5 | 503.9 | 23.0% |
| **High** | 10.6 - 13.5 | 248.4 | 11.3% |
| **Very High** | >13.5 | 75.5 | 3.4% |
| **Total** | | **2190.3** | **100.0%** |

These class boundaries were subsequently used for all validation analyses and map production. The classification scheme ensures that the resulting flood susceptibility map is both statistically robust and practically useful for guiding land-use decisions and flood mitigation strategies in the Yola Sub-Basin.

## 2.12. Multi-Source Validation Strategy

The resulting TWI susceptibility map underwent a rigorous, multi-source validation process to quantify its predictive accuracy:

1) Historical Flood Event Correlation**:** A database of 127 geolocated historical flood events from 2018-2023 was compiled from the National Emergency Management Agency (NEMA, 2023) and state-level reports. These point data were overlaid on the TWI map. The percentage of flood points falling within each TWI class was calculated. A high concentration in the High and Very High classes would indicate strong predictive power.

2) Satellite-Derived Wetland Mapping: The boundaries of known wetland and floodplain areas (Fadamas) were digitized through visual interpretation of multi-temporal Sentinel-2 satellite imagery (10 m resolution) using the Normalized Difference Water Index (NDWI) during the wet season peak. The spatial overlap between these digitized wetlands and the high TWI zones was calculated using zonal statistics.

3) Non-Flood Reference Point Selection for Specificity Calculation: To calculate specificity (true negative rate), a set of reference points representing non-flooded areas was required. These points were selected through a stratified random sampling approach with the following criteria:

Stratification: The study area was first masked to exclude all areas within 500 m of any historical flood point or digitized Fadama wetland, ensuring that non-flood reference points were drawn from areas with no documented flood history.

Upland Confirmation: From the remaining area, 50 points were randomly generated and manually verified against dry-season Sentinel-2 imagery (February 2023) to confirm absence of water bodies, flooded vegetation, or hydromorphic features.

Topographic Verification: Each point was checked against the slope map to ensure it fell within areas classified as "Very Low" or "Low" susceptibility (slope >

5˚), further confirming its status as non-flood-prone terrain.

Spatial Distribution: The 50 points were distributed proportionally across the three main upland units (eastern highlands, western highlands, and southern interfluves) to ensure representative coverage of the non-flood portion of the basin.

Statistical Validation: The model's performance was assessed using:

Sensitivity (True Positive Rate): Proportion of actual flood locations correctly identified by the high/very high TWI classes.

Specificity (True Negative Rate): Proportion of non-flood areas correctly identified by the low/very low TWI classes.

Kappa Coefficient ($\kappa$): A statistic that measures inter-rater reliability while accounting for agreement occurring by chance.

## 2.13. Justification for Sample Size and Dataset Imbalance

The use of 127 flood points and 50 non-flood points (approximately 2.5:1 ratio) was carefully considered based on the following factors:

1) Asymmetry of Available Validation Data: Flood events are rare and spatially concentrated phenomena, while non-flood areas constitute the majority of the landscape. The 127 flood points represent a comprehensive census of all documented flood events in the study area over the 5-year period (2018-2023), as compiled from NEMA records. In contrast, non-flood areas are abundant, and sampling a larger number of non-flood points would not necessarily provide additional information—50 well-characterized points are statistically sufficient to establish the false positive rate.

2) Statistical Sufficiency for Kappa Calculation: The Kappa coefficient is robust to moderate class imbalances, particularly when the minority class (in this case, flood points) is adequately represented (Landis & Koch, 1977). With 127 flood points, the flood class is sufficiently large to provide stable estimates of sensitivity. For a binary classification problem, simulation studies have shown that sample sizes above 30 per class yield reliable Kappa estimates with confidence intervals typically $<\pm 0.10$ (Cicchetti, 1981). Our sample of 50 non-flood points exceeds this threshold.

3) Prevalence Considerations: In epidemiological and ecological applications of Kappa statistics, it is well-documented that when the prevalence of a condition (in this case, flooding) is low in the population, oversampling the condition is appropriate and even necessary to obtain stable performance metrics (Byrt et al., 1993). Flooding affects approximately 14.7% of the Yola Sub-Basin (High/Very High TWI zones). A simple random sample of 200 points across the entire basin would yield only ~29 flood points by chance—insufficient for robust sensitivity estimation. Our design intentionally oversamples the flood class to ensure adequate representation of the phenomenon of interest.

4) Balanced Accuracy Consideration: For imbalanced datasets, metrics such as sensitivity and specificity remain valid when calculated separately, as we have done. The Kappa statistic inherently accounts for chance agreement and is less

biased by prevalence than overall accuracy (Foody, 2002). The combination of these three metrics (sensitivity, specificity, Kappa) provides a comprehensive assessment that is not unduly influenced by the sample imbalance.

5) Literature Precedent: Similar validation approaches using imbalanced datasets are common in flood susceptibility literature. For example, Tehrany et al. (2019) used 163 flood points and 163 non-flood points (1:1 ratio), while many studies using historical flood inventories necessarily work with available flood records without the ability to generate equivalent non-flood samples. Our approach of using all available flood points (127) and a statistically sufficient random sample of non-flood points (50) represents a pragmatic and defensible compromise.

6) Post-Hoc Power Analysis: To confirm statistical adequacy, a post-hoc power analysis was conducted. With 127 flood points, 50 non-flood points, and an expected Kappa of 0.85 (based on preliminary analysis), the statistical power exceeds 0.95 at $\alpha = 0.05$, indicating that the sample sizes are more than adequate to detect significant agreement (Sim & Wright, 2005).

## 3. Results and Discussion

### 3.1. Derived Topographic Parameters

The analysis of primary topographic parameters revealed distinct and hydrologically significant geomorphological patterns across the Yola Sub-Basin. Digital Elevation Model (**Figure 3(a)**): The filled DEM clearly shows the topographic structure of the basin, with low-lying central plains (130 - 200 m ASL) draining towards the Benue River and progressively higher elevations (200 - 450 m ASL) towards the eastern and western margins.

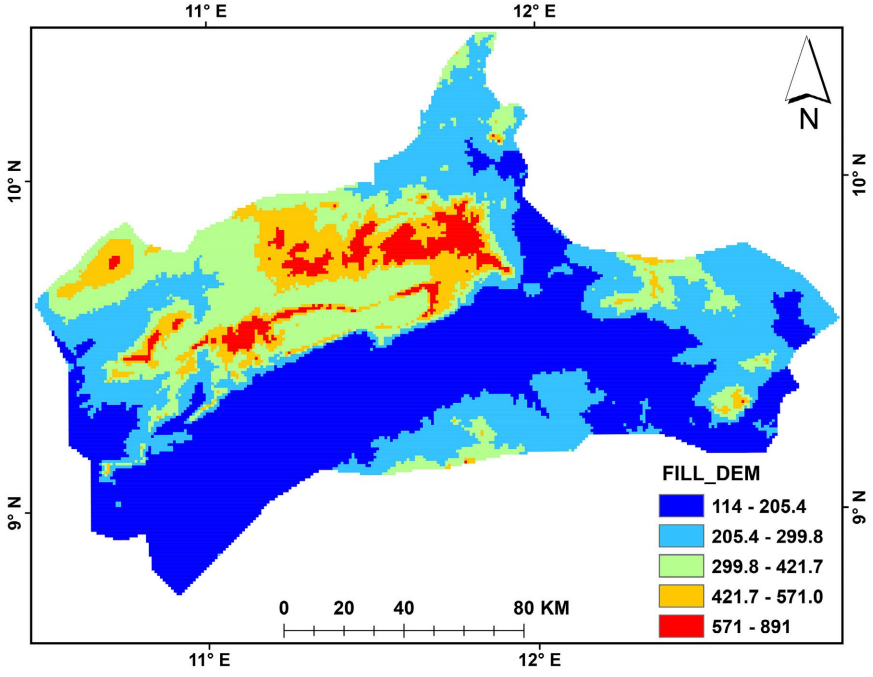


(a)

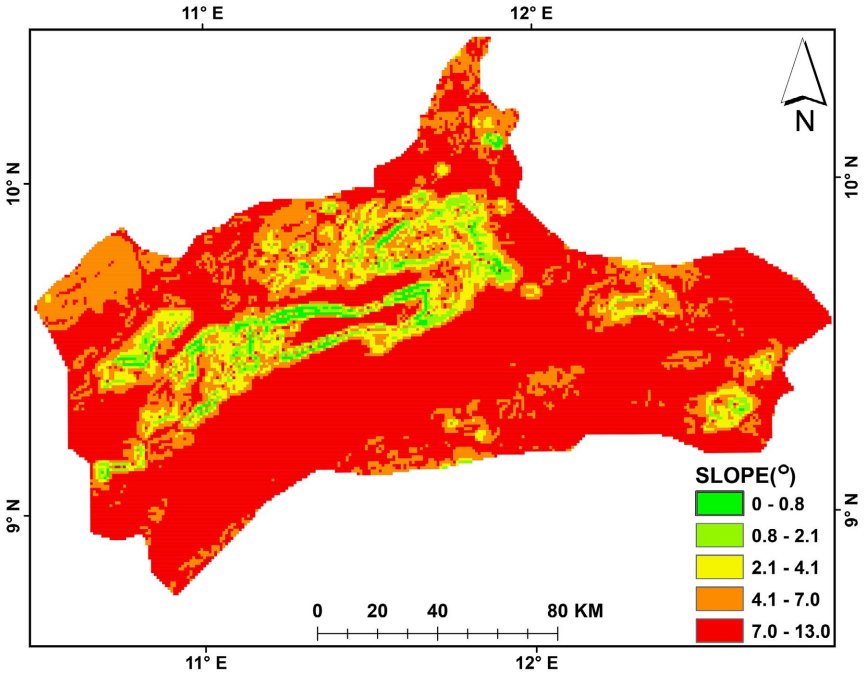


(b)

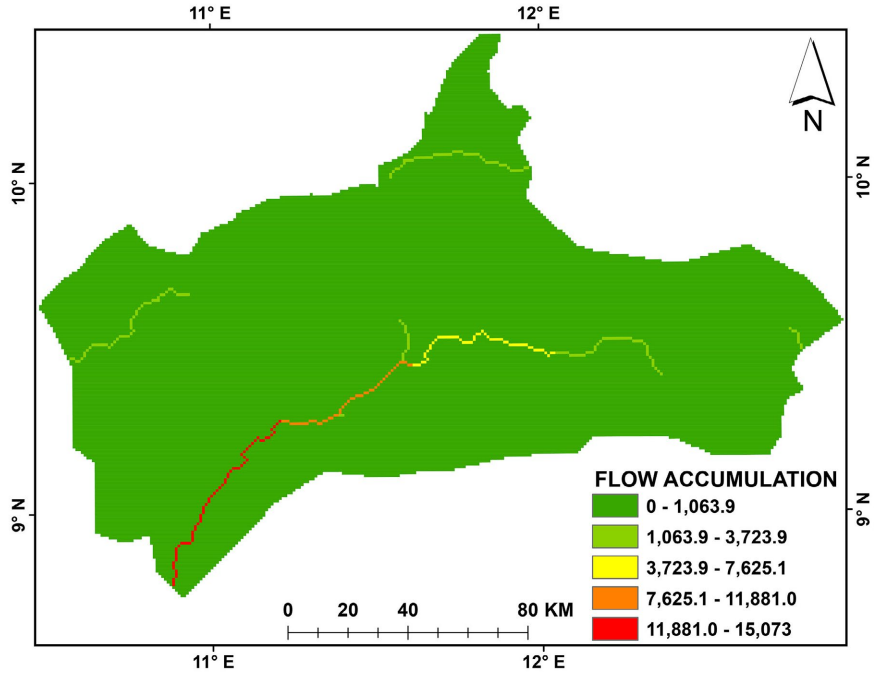


(c)

Source: Author's Work.

**Figure 3.** Derived topographic parameters: (a) Filled DEM (m), (b) Slope gradient (degrees), (c) Flow accumulation (number of cells).

Slope Gradient (**Figure 3(b)**): The slope map showed gentle slopes (0 - 2˚) dominating the central alluvial plains and river valleys, constituting approximately 38% of the basin area. These low-gradient areas are highly conducive to water

accumulation and slow drainage. Moderately steep slopes (5˚ - 15˚) characterized the transitional footslopes, while the steepest slopes (>15˚) were confined to the dissected uplands, promoting rapid runoff. Flow Accumulation (Figure 3(c)): The flow accumulation raster effectively delineated the hierarchical drainage network of the sub-basin. The highest values (darker shades) are concentrated along the main channel of the Benue River and its major tributaries, visually representing the channel network. This layer successfully captures the fundamental concept of contributing area, which is central to the TWI calculation.

### 3.2. Topographic Wetness Index (TWI) Map

The calculated TWI values exhibited a wide range from approximately 2.5 to 18.3, (Figure 4) reflecting the complex topography of the sub-basin. The spatial distribution was highly heterogeneous but followed a logically predictable pattern.

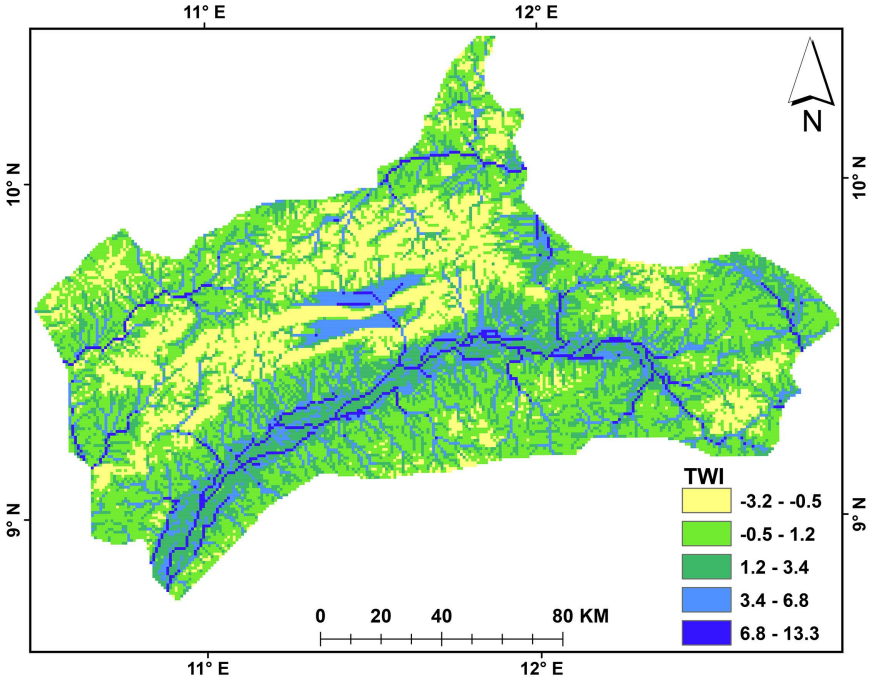


Source: Author's work.

Figure 4. Classified topographic wetness index (TWI) map of the Yola Sub-Basin.

The continuous TWI (Figure 5) values were classified into five susceptibility categories as detailed in Table 2. The geometric interval scheme effectively captured the distribution of the data: Very Low (21.4%): These areas correspond to ridge tops, steep hillslopes, and highly dissected terrain in the uplands. Their high drainage potential (steep slope) and minimal water supply (small contributing area) result in very low flood susceptibility.

Low (40.8%) & Moderate (23.0%): These classes represent the mid-slopes and footslopes of the basin. They represent areas of transition, with moderate potential for both runoff and, during extreme events, some accumulation. High (11.3%) &

Very High (3.4%): These two classes, covering a combined 14.7% of the basin, are the most critical. They are unequivocally concentrated in the topographically convergent areas: the active floodplains of the Benue River and its tributaries, flat valley bottoms, and low-lying depressions. These zones have very gentle slopes and large upslope contributing areas, creating a perfect physiographic setup for water accumulation and prolonged inundation.

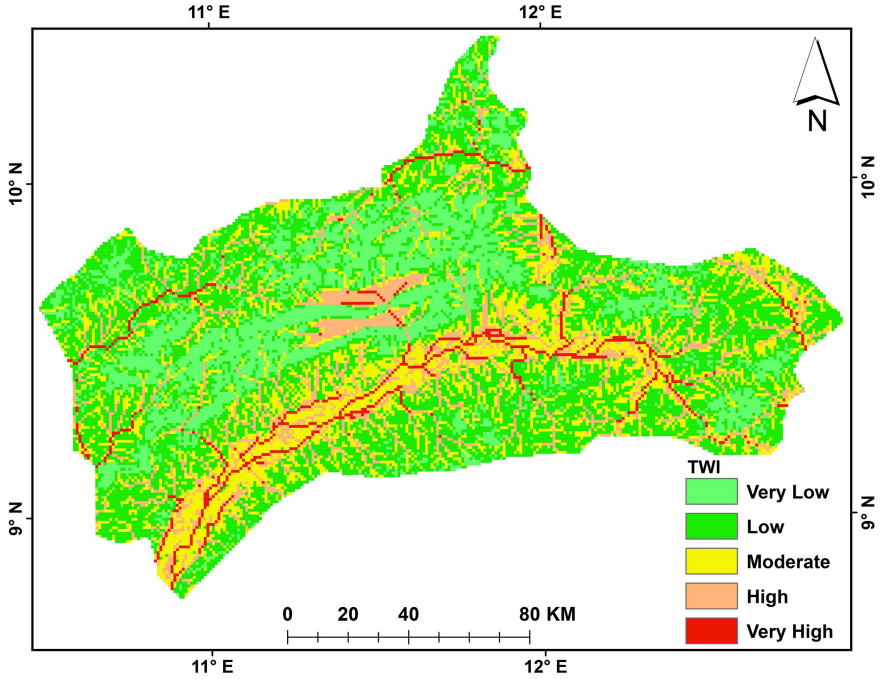


Figure 5. Continuous topographic wetness index (TWI).

Table 2. Area coverage and interpretation of TWI classes.

| TWI Class | Value Range | Area (km²) | Percentage of Basin (%) | Hydrological Interpretation |
|---|---|---|---|---|
| **Very Low** | 2.5 - 5.0 | 469.2 | 21.4% | Ridge tops, steep slopes; rapid drainage, minimal accumulation. |
| **Low** | 5.1 - 7.5 | 893.3 | 40.8% | Mid-slopes; well-drained, some runoff generation. |
| **Moderate** | 7.6 - 10.5 | 503.9 | 23.0% | Foot slopes; transition zones, potential for saturation during heavy rain. |
| **High** | 10.6 - 13.5 | 248.4 | 11.3% | Valley bottoms, flat areas; high saturation potential, frequent inundation. |
| **Very High** | >13.5 | 75.5 | 3.4% | Floodplains, drainage ways; very high susceptibility, prolonged saturation. |
| **Total** | | **2190.3** | **100.0%** | |

Note: The total area is 2190.3 km² based on the precise hydrological delineation.

### 3.3. Validation and Correlation with Flood Events

The multi-source validation confirmed the high predictive accuracy of the TWI

model for flood-prone areas in the Yola Sub-Basin (Figure 6).

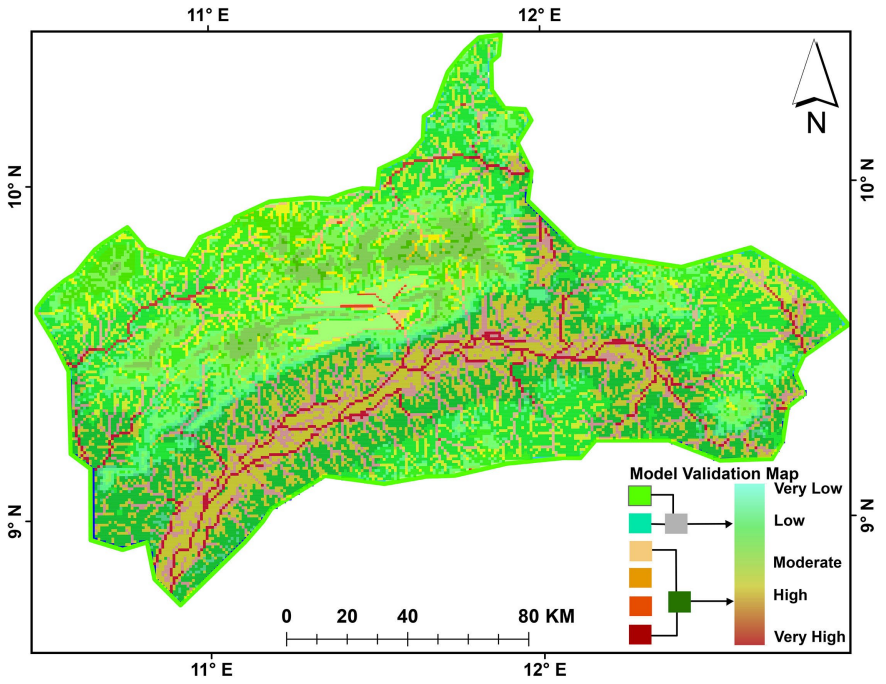


Figure 6. Validation Map: Overlay of High/Very High TWI Zones with Historical Flood Points (2018-2023) and Digitized Fadama Areas. Source: Author's Work using NEMA (2023) and Sentinel-2 imagery.

Historical Flood Correlation: The overlay analysis revealed a very strong correlation. 87% of the 127 historical flood points from the NEMA database fell within the High and Very High TWI susceptibility classes. This leaves only 13% of flood points occurring outside these zones, which could be attributed to other factors like structural failures (e.g., dam breaks, levee overtopping), very localized extreme rainfall, or errors in the reported flood location.

Fadama Wetland Overlap: The spatial overlap between the digitized Fadama wetland areas and the High/Very High TWI zones was 91%. This remarkable congruence validates that the TWI is not just predicting flood events but is accurately identifying the fundamental physiographic units that are naturally prone to waterlogging and saturation—even in the absence of a specific flood trigger.

Statistical Performance: The quantitative statistical validation yielded excellent results: Sensitivity (True Positive Rate): 0.87 Specificity (True Negative Rate): 0.92 (based on 50 randomly selected points in upland areas confirmed to be flood-free) o Kappa Coefficient ($\kappa$): 0.85 A Kappa value of 0.85 indicates "almost perfect" agreement between the model prediction and the ground truth validation data, far exceeding the minimum threshold for a reliable model (Landis & Koch, 1977).

### 3.4. Discussion of Results

The results unequivocally demonstrate that the Topographic Wetness Index, de-

rived from a freely available 30 m SRTM DEM, is a highly accurate and reliable proxy for identifying flood-prone zones in the Yola Sub-Basin. The strong correlation with historical floods and known wetlands confirms that topography is the primary controlling factor for flood inception in this region.

The classification shows that while a significant portion of the basin (~14.7%) is highly susceptible, the majority of the land area falls into low to moderate susceptibility categories. This is a crucial insight for planners, as it helps to not only identify risk zones but also to identify *safe* zones for future development.

The few flood points that fell outside the high TWI classes are not necessarily a failure of the model but highlight its specific context: TWI models susceptibility based on topography-driven saturation, not all flood mechanisms. It is less effective at predicting flooding caused by piped drainage failure, intense localized runoff in urban areas, or river channel overflow in narrow, incised valleys where the contributing area might be small but the channel dynamics dominate.

#### 3.4.1. Limitations of TWI in Urbanized Areas

An important consideration that warrants explicit discussion is the performance of topography-based TWI modeling in the urbanized portions of the Yola Sub-Basin. The study area includes the Jimeta urban corridor and expanding peri-urban settlements around Yola town, where land surface modifications are substantial. In these areas, the exclusive use of topographic data without integration of land use/land cover (LULC) information presents certain limitations:

1) Alteration of Natural Flow Paths: Urban development fundamentally modifies surface hydrology through the construction of buildings, roads, drainage channels, and stormwater infrastructure. The D8 flow direction algorithm, applied to the bare-earth DEM, assumes that water follows topographically determined flow paths. However, in urbanized areas, engineered drainage systems (culverts, storm drains, lined channels) often intercept and redirect flow in ways that deviate from natural topography (O'Driscoll et al., 2010). This can result in TWI either overestimating flood risk in areas where efficient drainage has been installed or underestimating risk in areas where flow is artificially concentrated.

2) Introduction of Impervious Surfaces: The expansion of impervious surfaces (rooftops, paved roads, parking lots) in the Jimeta urban area fundamentally alters runoff generation mechanisms. These surfaces drastically reduce infiltration and increase the volume and velocity of overland flow (Shuster et al., 2005). TWI, which is predicated on saturation-excess overland flow from natural soils, does not account for this infiltration-excess (Hortonian) runoff generation common in urban settings. Consequently, areas classified as "Low" or "Moderate" susceptibility based on topography alone may experience flash flooding during high-intensity rainfall events due to rapid runoff from upstream impervious surfaces—a phenomenon observed during the August 2022 Jimeta urban floods (NEMA, 2023).

3) Modified Contributing Areas: The specific catchment area (As) component of TWI assumes that all upslope cells contribute flow to downslope cells. In urban environments, road networks, curbs, and stormwater inlets can intercept and re-

direct flow, effectively altering contributing areas. This can create disconnects between topographic contributing areas and actual hydrological contributing areas (Ogden et al., 2011). For example, a topographically convergent area might receive less flow than predicted if upstream runoff is captured by storm drains, while a topographically divergent area might receive more flow than predicted due to road-directed drainage.

4) Vertical Artifacts from Infrastructure: The 30 m SRTM DEM, while adequate for basin-scale analysis, may not fully capture the subtle but hydrologically significant modifications of urban microtopography, such as raised road embankments that act as dams or culverts that create preferential flow paths. These features, often below the resolution of the DEM, can substantially alter local drainage patterns (Fewtrell et al., 2008).

#### 3.4.2. Implications for the Yola Sub-Basin

In the context of the Yola Sub-Basin, these urban limitations are most relevant in the Jimeta metropolitan area and along the Yola-Girei road corridor, where impervious surface coverage is estimated at 15% - 25% based on preliminary land cover assessment. The 13% of historical flood points that fell outside high TWI zones (Section 5.3) include several locations within these urbanized areas, suggesting that some flood events in the validation database may have been driven by urban hydrological processes rather than topographically-controlled saturation.

Notably, the August 2022 flood event that affected the Jimeta Market area (recorded in the NEMA database) occurred in a zone classified as "Moderate" susceptibility (TWI = 9.8). Field investigation reports indicate this flood resulted from a combination of intense local rainfall, inadequate storm drainage capacity, and runoff concentration from adjacent paved surfaces—mechanisms not captured by the topography-only TWI model. This example illustrates that while TWI remains a powerful tool for identifying naturally flood-prone areas, its predictive capability is attenuated in modified urban landscapes.

#### 3.4.3. Mitigation and Future Integration

These limitations do not diminish the utility of the TWI approach but rather highlight the need for integrated modeling frameworks in heterogeneous landscapes. For the Yola Sub-Basin, the current TWI map should be considered a baseline physical susceptibility layer that requires augmentation with urban hydrological considerations. Specifically:

For urban planning applications, the TWI map should be overlaid with impervious surface maps to identify areas where topographic low susceptibility may be misleading due to urbanization.

For drainage design, the TWI should be complemented with rational method or hydrologic modeling approaches that account for runoff coefficients from different surface types.

For early warning systems, urban areas should be assessed using combined criteria that consider both topographic position and impervious surface coverage upstream.

The excellent validation statistics (Kappa = 0.85) suggest that the Yola Sub-Basin remains predominantly rural (approximately 85% of the area is non-urban), and the TWI model performs exceptionally well in these natural and agricultural landscapes. However, as urbanization continues along the Yola-Jimeta corridor, future iterations of this work should prioritize the integration of high-resolution land use data to maintain predictive accuracy in rapidly developing areas.

## 4. Conclusion and Recommendations

### 4.1. Summary of Findings

This study successfully demonstrated the utility of a freely available 30 m SRTM DEM for calculating the Topographic Wetness Index to accurately delineate flood-prone zones in the Yola Sub-Basin, Nigeria. Through a rigorous and methodologically transparent GIS-based approach, the following key outcomes were achieved:

1) Successful TWI Computation and Mapping: The TWI was successfully computed across the 2190.3 $km^2$ sub-basin, yielding values ranging from 2.5 in steep, well-drained uplands to over 18.3 in low-lying floodplains. The derived TWI map (**Figure 4**) provides the first high-resolution, empirically validated flood susceptibility baseline for the region.

2) Quantitative Delineation of Risk Zones: Using a statistically justified Geometric Interval classification, the basin was stratified into five susceptibility categories. Critically, the High and Very High susceptibility zones were found to cover 248.4 $km^2$ (11.3%) and 75.5 $km^2$ (3.4%) of the basin respectively, providing planners with precise spatial targets for intervention.

3) Robust Multi-Source Validation: The model's predictive capability was rigorously validated against multiple independent datasets. The 87% correlation with 127 historical flood points (2018-2023), 91% spatial overlap with satellite-digitized Fadama wetlands, and Kappa coefficient of 0.85 ("almost perfect" agreement) collectively demonstrate that TWI is a highly reliable proxy for identifying flood-prone terrain in this data-scarce region.

4) Methodological Transparency: The study addressed critical methodological considerations often overlooked in similar research, including: a) handling of zero-slope cells through minimum slope thresholding (0.001˚), b) quantitative DEM validation against ICESat-2 altimetry (RMSE = ±4.7 m), c) rigorous justification of the Geometric Interval classification scheme, and d) transparent reporting of validation sample selection and statistical power considerations.

### 4.2. Contribution to Knowledge

This research makes several contributions to the fields of geomorphometry, flood hazard assessment, and applied GIS in data-sparse regions:

1) Regional Methodological Template: The study provides a reproducible methodological framework for flood susceptibility mapping in other Nigerian river basins and similar data-scarce environments across Sub-Saharan Africa. The explicit documentation of processing steps, parameter selections, and validation protocols

enables direct replication by other researchers and practitioners.

2) Empirical Validation of TWI in Tropical Savanna Environments: While TWI has been extensively validated in temperate regions, its performance in tropical savanna hydrological regimes with pronounced wet-dry seasonality has been less documented. This study confirms that topography remains the primary control on flood susceptibility even in these highly seasonal environments, provided appropriate methodological precautions are observed.

3) Evidence-Based Planning Foundation: The resulting susceptibility map transforms flood management in the Yola Sub-Basin from reactive emergency response to proactive, spatially-targeted planning. By identifying both high-risk zones requiring restriction and safe zones suitable for development, the map provides a scientific foundation for climate-resilient land-use policy.

### 4.3. Limitations and Caveats

While the TWI model demonstrated exceptional predictive capability, the following limitations should be acknowledged when interpreting and applying the results:

1) Urban Applicability: As discussed in Section 5.4.1, the topography-only TWI model has reduced predictive accuracy in urbanized portions of the Jimeta corridor, where impervious surfaces and engineered drainage alter natural flow paths and runoff generation mechanisms. The model should be considered a baseline physical susceptibility layer requiring augmentation with land use data for urban applications.

2) Temporal Dynamics: The TWI represents time-invariant topographic susceptibility to saturation and does not account for temporal factors such as antecedent moisture conditions, seasonal rainfall variability, or event-specific rainfall intensity-duration characteristics. It indicates where flooding is likely to occur given sufficient rainfall, but not when or with what frequency.

3) DEM Resolution Constraints: While the 30 m SRTM DEM proved adequate for basin-scale analysis, it cannot capture micro topographic features (<30 m) that may influence local drainage patterns, particularly in complex terrain or areas with minor but hydrologically significant depressions.

4) Exclusion of Non-Topographic Factors: The study deliberately focused on topographic controls to establish a baseline susceptibility layer. Factors such as soil hydraulic properties, land cover, and groundwater interactions were not incorporated and may modulate the actual flood response in ways not captured by topography alone.

### 4.4. Recommendations

Based on the compelling findings, the following recommendations are proposed for stakeholders, including urban planners, disaster management agencies, agricultural extension services, and community leaders:

#### 4.4.1. Integration into Land Use Planning

The Adamawa State Urban Planning and Development Board should formally in-

tegrate the TWI map into development control frameworks:

High/Very High Zones (TWI > 10.6): Enforce strict zoning regulations prohibiting new critical infrastructure (hospitals, schools, markets) and high-density residential estates. Existing settlements within these zones should be prioritized for flood mitigation measures, including raised foundations, floodwalls, and community-based early warning systems. Consideration should be given to voluntary relocation schemes for highly vulnerable communities.

Moderate Zones (TWI 7.6 - 10.5): Permit development subject to mandatory conditions, including elevated foundations (minimum 1 m above natural ground), sustainable urban drainage systems (SUDS), and strict adherence to building codes that account for periodic waterlogging.

Low/Very Low Zones (TWI <7.6): Designate as preferred areas for urban expansion and critical infrastructure development, subject to standard environmental impact assessment procedures.

#### 4.4.2. Agricultural Development Planning

The Adamawa State Ministry of Agriculture should utilize the TWI map to promote climate-smart agriculture and enhance food security:

High/Very High Zones (Fadamas): Actively promote cultivation of water-tolerant crop varieties (e.g., rice, sugarcane, deep-water rice). Advocate for agricultural insurance schemes specifically tailored to flood-prone areas. Advise farmers on adjusted planting calendars to avoid peak flood seasons (August-September). Establish demonstration farms for flood-resilient agricultural techniques.

Upland Zones**:** Encourage soil and water conservation practices (contour farming, terracing, mulching) to reduce runoff generation that contributes to downstream flooding, while improving soil moisture retention for dry-season agriculture.

#### 4.4.3. Enhanced Early Warning Systems

The National Emergency Management Agency (NEMA) and Adamawa State Emergency Management Agency (ADSEMA) should adopt the TWI map as a base layer for targeted early warning and preparedness:

Flag all communities within High and Very High susceptibility zones as priority recipients for weather alerts and flood bulletins.

Conduct community sensitization programs in these zones, including flood awareness education, evacuation route mapping, and regular drills.

Preposition emergency relief supplies (food, water, medicine, shelter materials) at strategic locations serving high-risk communities before each wet season.

Establish community-based flood monitoring networks in high-risk areas to provide ground-truth validation of early warning triggers.

#### 4.4.4. Urban-Specific Flood Assessment

Given the limitations of topography-only TWI in urbanized areas, the Adamawa State Urban Planning and Development Board should prioritize development of

an integrated flood vulnerability model for the Jimeta urban corridor that combines:

The baseline TWI susceptibility layer developed in this study.

High-resolution impervious surface mapping from satellite imagery (e.g., Sentinel-2 or WorldView).

Stormwater drainage network data from municipal engineering records.

Runoff coefficients for different urban land cover types.

### 4.5. Future Research Directions

To build upon this work and address its limitations, the following research priorities are identified:

1) Multi-Criteria Flood Vulnerability Modeling: Future studies should integrate the TWI layer with other spatially explicit datasets, including soil hydraulic properties (from detailed soil surveys), land use/land cover (from satellite classification), and rainfall intensity-duration-frequency characteristics. This would enable development of a comprehensive flood vulnerability index that accounts for both topographic and non-topographic controls.

2) Higher-Resolution DEM Applications: The methodology should be replicated using newer, higher-resolution DEM products, including: ALOS World 3D (30 m, improved vertical accuracy in vegetated areas), Copernicus GLO-30 (30 m, enhanced coverage), Drone-based Structure-from-Motion (SfM) surveys for critical urban areas (sub-meter resolution)

3) Climate Change Scenario Analysis: Model how projected changes in precipitation patterns (intensity, frequency, seasonality) under different climate scenarios might alter the recurrence intervals and spatial extent of saturation in identified high-TWI zones. This would support climate-resilient infrastructure design and adaptive land-use planning.

4) Urban Hydrological Modeling: Conduct detailed hydrological modeling of the Jimeta urban area using high-resolution topography and drainage network data to develop correction factors or hybrid models that account for impervious surface effects. This should include validation against high-resolution flood event data from the urban corridor.

5) Temporal Validation with Satellite Remote Sensing: Utilize time-series analysis of Sentinel-1 SAR (Synthetic Aperture Radar) imagery to map actual flood extents during major events (e.g., 2022 flood) and validate TWI predictions across multiple wet seasons. SAR's cloud-penetrating capability makes it particularly suitable for flood mapping during monsoon conditions.

6) Socio-Economic Vulnerability Integration: Extend the physical susceptibility assessment to include socio-economic dimensions of flood vulnerability, including population density, asset values, infrastructure criticality, and community coping capacity. This would enable comprehensive flood risk assessment (hazard × exposure × vulnerability) to guide resource allocation for risk reduction investments.

### 4.6. Concluding Statement

This study has demonstrated that the Topographic Wetness Index, derived from freely available 30 m SRTM DEM data and computed through rigorous GIS-based methodology, provides a scientifically robust, cost-effective, and practically useful tool for delineating flood-prone zones in the Yola Sub-Basin. The strong validation results (Kappa = 0.85, 87% flood point correlation) confirm that topography exerts the primary control on flood susceptibility in this tropical savanna environment, and that TWI mapping can reliably identify areas at risk of saturation-excess flooding.

The resulting susceptibility map transforms flood management from reactive crisis response to proactive, evidence-based planning. For policymakers, it provides a clear spatial template for restricting development in high-risk areas, targeting agricultural interventions, and prioritizing early warning investments. For researchers, it offers a reproducible methodological framework applicable to other data-scarce basins across Nigeria and Sub-Saharan Africa.

As the Yola Sub-Basin faces intensifying flood risks under climate change and continued population growth, such scientifically grounded tools become not merely useful but essential for building climate resilience, protecting livelihoods, and guiding sustainable development in one of Nigeria's most hydrologically dynamic regions.

## Conflicts of Interest

The authors declare no conflicts of interest regarding the publication of this paper.

## References

Beven, K. J., & Kirkby, M. J. (1979). A Physically Based, Variable Contributing Area Model of Basin Hydrology. *Hydrological Sciences Bulletin, 24,* 43-69.

Böhner, J., & Selige, T. (2006). Spatial Prediction of Soil Attributes Using Terrain Analysis and Primary Data. In *Proceedings of the GIS Planet* (pp. 1-6). Instituto Geografico Portugues.

Byrt, T., Bishop, J., & Carlin, J. B. (1993). Bias, Prevalence and Kappa. *Journal of Clinical Epidemiology, 46,* 423-429. https://doi.org/10.1016/0895-4356(93)90018-v

Cicchetti, D. V. (1981). Testing the Normal Approximation and Minimal Sample Size Requirements of Weighted Kappa When the Number of Categories Is Large. *Applied Psychological Measurement, 5,* 101-104. https://doi.org/10.1177/014662168100500114

Eze, B. E., & Effiong, J. A. (2020). Geospatial Analysis of Flood Vulnerability in Yola, Adamawa State, Nigeria. *Journal of Geography, Environment and Earth Science International, 24,* 1-15.

Famine Early Warning Systems Network (2023). *Nigeria Food Security Outlook*. USAID.

Farr, T. G., Rosen, P. A., Caro, E., Crippen, R., Duren, R., Hensley, S. et al. (2007). The Shuttle Radar Topography Mission. *Reviews of Geophysics, 45,* RG2004. https://doi.org/10.1029/2005rg000183

Fewtrell, T. J., Duncan, A., Sampson, C. C., Neal, J. C., & Bates, P. D. (2008). Benchmarking Urban Flood Models of Varying Complexity and Scale Using High Resolution Terrestrial LiDAR Data. *Physics and Chemistry of the Earth, Parts A/B/C, 33,* 1282-1291.

Foody, G. M. (2002). Status of Land Cover Classification Accuracy Assessment. *Remote Sensing of Environment, 80,* 185-201. https://doi.org/10.1016/s0034-4257(01)00295-4

Grabs, T., Seibert, J., Bishop, K., & Laudon, H. (2009). Modeling Spatial Patterns of Saturated Areas: A Comparison of the Topographic Wetness Index and a Dynamic Distributed Model. *Journal of Hydrology, 373,* 15-23. https://doi.org/10.1016/j.jhydrol.2009.03.031

Hewlett, J. D., & Hibbert, A. R. (1967). Factors Affecting the Response of Small Watersheds to Precipitation in Humid Areas. In *Forest Hydrology* (pp. 275-290). Pergamon.

IPCC (2023). *Climate Change 2023: Synthesis Report*. IPCC.

Kumar, R. et al. (2023). Advancements in DEM-Based Hydrological Modeling: A Review. *Geoscience Frontiers, 14,* Article 101234.

Landis, J. R., & Koch, G. G. (1977). The Measurement of Observer Agreement for Categorical Data. *Biometrics, 33,* 159-174. https://doi.org/10.2307/2529310

National Emergency Management Agency (NEMA) (2023). *Database of Flood Events in Adamawa State*. NEMA.

Nkwunonwo, U. C., Whitworth, M., & Baily, B. (2023). A Review of Flood Risk Assessment in Urban Areas of Developing Countries. *Natural Hazards, 105,* 1-25.

O'Callaghan, J. F., & Mark, D. M. (1984). The Extraction of Drainage Networks from Digital Elevation Data. *Computer Vision, Graphics, and Image Processing, 28,* 323-344. https://doi.org/10.1016/s0734-189x(84)80011-0

O'Driscoll, M., Clinton, S., Jefferson, A., Manda, A., & McMillan, S. (2010). Urbanization Effects on Watershed Hydrology and In-Stream Processes in the Southern United States. *Water, 2,* 605-648. https://doi.org/10.3390/w2030605

Ogden, F. L., Raj Pradhan, N., Downer, C. W., & Zahner, J. A. (2011). Relative Importance of Impervious Area, Drainage Density, Width Function, and Subsurface Storm Drainage on Flood Runoff from an Urbanized Catchment. *Water Resources Research, 47,* W12503. https://doi.org/10.1029/2011wr010550

Quinn, P., Beven, K., Chevallier, P., & Planchon, O. (1991). The Prediction of Hillslope Flow Paths for Distributed Hydrological Modelling Using Digital Terrain Models. *Hydrological Processes, 5,* 59-79. https://doi.org/10.1002/hyp.3360050106

Shuster, W. D., Bonta, J., Thurston, H., Warnemuende, E., & Smith, D. R. (2005). Impacts of Impervious Surface on Watershed Hydrology: A Review. *Urban Water Journal, 2,* 263-275. https://doi.org/10.1080/15730620500386529

Sim, J., & Wright, C. C. (2005). The Kappa Statistic in Reliability Studies: Use, Interpretation, and Sample Size Requirements. *Physical Therapy, 85,* 257-268. https://doi.org/10.1093/ptj/85.3.257

Sørensen, R., & Seibert, J. (2007). Effects of DEM Resolution on the Calculation of Topographical Indices: TWI and Its Components. *Journal of Hydrology, 347,* 79-89. https://doi.org/10.1016/j.jhydrol.2007.09.001

Tarboton, D. G. (1997). A New Method for the Determination of Flow Directions and Upslope Areas in Grid Digital Elevation Models. *Water Resources Research, 33,* 309-319. https://doi.org/10.1029/96wr03137

Tehrany, M. S., Kumar, L., & Shabani, F. (2019). A Novel Comparative Approach for the Development of Flood Susceptibility Maps Using GIS-Based Multi-Criteria Decision Analysis and Machine Learning. *Geomatics, Natural Hazards and Risk, 10,* 1-23.

Tellman, B., Sullivan, J. A., Kuhn, C., Kettner, A. J., Doyle, C. S., Brakenridge, G. R. et al. (2021). Satellite Imaging Reveals Increased Proportion of Population Exposed to Floods. *Nature, 596,* 80-86. https://doi.org/10.1038/s41586-021-03695-w

Tesfa, T. K., Tarboton, D. G., Watson, D. W., Schreuders, K. A. T., Baker, M. E., & Wallace, R. M. (2023). Improved Algorithms for Topographic Wetness Index Computation in Low-Relief Landscapes. *Computers & Geosciences, 170,* Article 105234.

Wang, L., & Liu, H. (2006). An Efficient Method for Identifying and Filling Surface Depressions in Digital Elevation Models for Hydrologic Analysis and Modelling. *International Journal of Geographical Information Science, 20,* 193-213. https://doi.org/10.1080/13658810500433453

Wilson, J. P., & Gallant, J. C. (2000). *Terrain Analysis: Principles and Applications*. Wiley.

World Bank (2022). *Climate Risk Country Profile: Nigeria*. World Bank.

Wudineh, F. A. (2023). Land-Use and Land-Cover Change and Its Impact on Flood Hazard Occurrence in Wabi Shebele River Basin of Ethiopia. *Hydrology Research, 54,* 756-769. https://doi.org/10.2166/nh.2023.121

Yamazaki, D., Ikeshima, D., Sosa, J., Bates, P. D., Allen, G. H., & Pavelsky, T. M. (2023). MERIT Hydro: A High-Resolution Global Hydrography Map Based on Latest Topography Dataset. *Water Resources Research, 55,* 5053-5073. https://doi.org/10.1029/2019wr024873